A robust scheme for compressible flows with a minimum artificial stabilization

By S. Kang AND H. Pitsch

1. Motivation and objective

The objective of the present study is to implement a robust numerical scheme for compressible flows that requires minimum artificial stabilization techniques. The lack of numerical stability is an issue often encountered in DNS/LES of compressible flows at high Reynolds number. In incompressible flows, the kinetic energy is theoretically conserved in the limit of high Reynolds number (i.e., zero viscosity). Using this property, very robust numerical schemes have been developed (Morinishi *et al.* 1998, 2004) that show an excellent stability in various flow regimes. In contrast, there is no such conserved quantity in compressible flows. Thus, most studies on turbulent compressible flows published so far employed various stabilization techniques such as artificial dissipation, filtering and dissipative discretization. However, these techniques are possibly disadvantageous in several aspects: 1) suppression of acoustic waves; 2) existence of artificial parameters; 3) lack of a physical meaning. The first issue is particularly important in the study of aeroacoustics. The second issue has a practical importance because correct physical insights as well as some experience are necessary in order to obtain a satisfactory solution for a particular flow with artificial stabilization via a proper selection of the parameters.

In order to address these issues, there have been recent studies that show a possibility of DNS/LES without or a minimum amount of artificial stabilization. Honein (2005) proposed using the entropy instead of the total energy or enthalpy as a conserved scalar in the governing equation set. Subbareddy & Candler (2009) presented a method to eliminate an error in the kinetic energy from the temporal discretization. Both methods reported an improved stability compared with existing ones especially at high Reynolds numbers.

These two methods pose different approaches but have similarities in two aspects: 1) preventing the convective/advective terms from spuriously affecting a volume-integrated transported quantity, which is a sign of numerical stability; 2) employing discretized operators similar to their analytic counterparts. In the present study, these two methods and a few other schemes are combined to provide superior stability compared to the existing schemes, as observed in our numerical tests.

2. Numerical methods

2.1. *Background*

It is a widely accepted idea that the non-linear convective/advective terms in the transport equations are the major sources of numerical instabilities. Thus, it is worthwhile to investigate their effect in an analytic sense. In the limit of zero viscosity and diffusivity, the transport equations for the momentum, energy and entropy are written as

$$\frac{\partial \rho u_i}{\partial t} + \frac{\partial \rho u_j u_i}{\partial x_j} + \frac{\partial p}{\partial x_i} = 0, \tag{2.1}$$

$$\frac{\partial \rho E}{\partial t} + \frac{\partial u_j \left(\rho E + p\right)}{\partial x_j} = 0, \tag{2.2}$$

$$\frac{\partial \rho e}{\partial t} + \frac{\partial \rho u_j e}{\partial x_j} + p\frac{\partial u_j}{\partial x_j} = 0, \tag{2.3}$$

$$\frac{\partial \rho s}{\partial t} + \frac{\partial \rho u_j s}{\partial x_j} = 0, \tag{2.4}$$

where t is the time, u_i is the velocity component in the i direction, p is the pressure, ρ is the density, E $(= e + u_i u_i/2)$ is the total energy, e is the internal energy, and s is the entropy. When multiplied by the conserved variable and arranged, these equations become

$$\frac{\partial \rho u_i^2}{\partial t} + \frac{\partial \rho u_j u_i^2}{\partial x_j} + 2\frac{\partial p u_i}{\partial x_i} - 2p\frac{\partial u_i}{\partial x_i} = 0, \tag{2.5}$$

$$\frac{\partial \rho E^2}{\partial t} + \frac{\partial \rho u_j E^2}{\partial x_j} + 2\frac{\partial E p u_j}{\partial x_j} - 2p u_j \frac{\partial E}{\partial x_j} = 0, \tag{2.6}$$

$$\frac{\partial \rho e^2}{\partial t} + \frac{\partial \rho u_j e^2}{\partial x_j} + 2\frac{\partial e p u_j}{\partial x_j} - 2u_j \frac{\partial e p}{\partial x_j} = 0, \tag{2.7}$$

$$\frac{\partial \rho s^2}{\partial t} + \frac{\partial \rho u_j s^2}{\partial x_j} = 0. \tag{2.8}$$

An important recognition by several previous studies (e.g., Morinishi *et al.* 1998, 2004; Honein 2005; Subbareddy & Candler 2009) is that the second and third terms are conservative and vanish when integrated over a periodic domain or a domain with no-slip walls. The first term integrated over the domain is regarded as a sign of stability because the integrated squared variable is bounded only if the entire field is bounded.† Thus, except for the total and internal energy equations, the convective/advective term should not affect the temporal change of the integrated squared variable.

This observation is valuable because it can remove the negative effect of the convective terms. However, it is not easy to maintain this feature in the discretized versions of these equations. In the present study, we combined several approaches to provide a similar stability as theoretically predicted from the analytic equations. They will be described in following sections.

2.2. *Staggered variables in space and time*

In the present study, variables are staggered in space and time, following the approaches of Pierce (2001) and Wall *et al.* (2002). Each component of the velocity is staggered by one half grid with respect to the scalars and each scalar is staggered by one half of the time step with respect to the velocities. As noted by Pierce, the staggered arrangement leads to a more accurate and stable discretization of the time-dependent continuity equation. The key advantage of the staggering is that it helps reducing grid-by-grid and step-by-step

† An important requirement is the physical feasibility - the positivity of density, pressure, etc.

oscillations by removing null modes of the size of Δx and Δt present in the discretization in a non-staggered arrangement.

2.3. *Choice of the energy variable*

A component for improved stability is the use of the entropy equation Eq. (2.4) instead of the total energy equation Eq. (2.2), as proposed by Honein (2005). As discussed by Honein, a weakness of the total energy equation is that the pressure part of the advective term does not provide sufficient stability for high Reynolds number. In contrast, by using Eq. (2.4), the integrated squared value is conserved as shown in Eq. (2.8), which leads to improved stability.

Let us discuss other features of the energy variables. Although the entropy Eq. (2.4) is inherently more stable than the other forms in the previous section, the situation may change in more complex problems. For example, in case of multi-component mixing and reaction problems, the additional source term for the entropy equation is more complex than the other forms of the energy equation, which makes other variables more attractive.

In case of the internal energy equation Eq. (2.3), it is observed that the stability of the momentum equation Eq. (2.1) is governed by the temporal change of the energy integral:

$$\frac{\partial}{\partial t}\left(\iiint \frac{\rho u_i^2}{2} dV\right) = \iiint p\frac{\partial u_i}{\partial x_i} dV = -\frac{\partial}{\partial t}\left(\iiint \rho e dV\right). \tag{2.9}$$

Thus, when Eqs. (2.1) and (2.5) are discretely consistent and the internal energy is discretely conserved, a stable solution of Eq. (2.3) leads to a stable solution of the momentum equation without additional stabilization. Spatial discretization satisfying these requirements is described in section 2.5. Although the internal energy Eq. (2.3) is not as robust as the entropy Eq. (2.4), a sufficient stabilization for Eq. (2.3) can remove the need for additional stabilization for the momentum equation.

Another issue is the discrete consistency between the total energy E and internal energy e in case of the staggered variable arrangement. In order to maintain the discrete consistency between the total energy Eq. (2.2) and the internal energy Eq. (2.3) in the staggered mesh, the following relationship is used:

$$E_{cv} = e_{cv} + \frac{1}{2\rho_{cv}}\left(\widetilde{\rho u_1^2} + \widetilde{\rho u_2^2} + \widetilde{\rho u_3^2}\right), \tag{2.10}$$

where $\widetilde{\ }$ denotes an interpolation from the faces (where u_i is located) to the center of a grid (denoted by cv). Frequently used relationships are

$$E_{cv} = e_{cv} + \frac{1}{2}\widetilde{u_i}\widetilde{u_i}, \tag{2.11}$$

$$E_{cv2} = e_{cv} + \frac{1}{2}\frac{\widetilde{\rho u_i}}{\rho_{cv}}\frac{\widetilde{\rho u_i}}{\rho_{cv}} \tag{2.12}$$

which are somewhat different. In practice, Eq. (2.10) is restrictive because the same interpolation is used for the pressure work and viscous dissipation terms to maintain consistency. Eqs. (2.10)−(2.12) are compared in a numerical test described below.

2.4. *Temporal discretization with a conservation property*

The present study employs a temporal discretization that shares a feature with the analytic temporal derivative. It is a minor modification of the method by Subbareddy &

Candler (2009) and Morinishi (2010). This method was motivated by an observation:

$$2u_i\left[\frac{\partial \rho u_i}{\partial t}+\frac{\partial \rho u_j u_i}{\partial x_j}\right]=\frac{\partial \rho u_i^2}{\partial t}+\frac{\partial \rho u_j u_i^2}{\partial x_j}. \tag{2.13}$$

However, with the Crank-Nicolson method in time

$$\begin{aligned}
&2u_i^m\left[\frac{\rho^{n+1}u_i^{n+1}-\rho^n u_i^n}{\Delta t}+\frac{\partial \rho u_j^m u_i^m}{\partial x_j}\right]\\
&=\frac{\rho^{n+1}\left(u_i^{n+1}\right)^2-\rho^n\left(u_i^n\right)^2}{\Delta t}+\frac{\partial \rho u_j^m\left(u_i^m\right)^2}{\partial x_j}+\frac{\rho^{n+1}-\rho^n}{\Delta t}u_i^n u_i^{n+1}+\frac{\partial \rho u_j^m}{\partial x_j}u_i^m u_i^m\\
&=\frac{\rho^{n+1}\left(u_i^{n+1}\right)^2-\rho^n\left(u_i^n\right)^2}{\Delta t}+\frac{\partial \rho u_j^m\left(u_i^m\right)^2}{\partial x_j}+\frac{\rho^{n+1}-\rho^n}{\Delta t}\left(\frac{u_i^{n+1}-u_i^n}{2}\right)^2,
\end{aligned} \tag{2.14}$$

where $u_i^m=\left(u_i^{n+1}+u_i^n\right)/2$. The last line of this equation is similar to the analytic counterpart Eq. (2.13) but has an additional term. In Eq. (2.13), $\iiint \rho u_i^2 dV$ is not affected by the non-linear term. In Eq. (2.14), however, the third term, which is regarded as a temporal error, can affect $\iiint \rho u_i^2 dV$. Thus, the original Crank-Nicolson method does not have the feature of the analytic derivative.

In the modified method by Subbareddy & Candler (2009) and Morinishi (2010), a different definition of the mid-time velocity u_i^m is used:

$$u_i^m=\frac{\sqrt{\rho^{n+1}}u_i^{n+1}+\sqrt{\rho^n}u_i^n}{\sqrt{\rho^{n+1}}+\sqrt{\rho^n}}. \tag{2.15}$$

Then, Eq. (2.14) becomes

$$\begin{aligned}
&2u_i^m\left[\frac{\rho^{n+1}u_i^{n+1}-\rho^n u_i^n}{\Delta t}+\frac{\partial \rho u_j^m u_i^m}{\partial x_j}\right]\\
&=\frac{\rho^{n+1}\left(u_i^{n+1}\right)^2-\rho^n\left(u_i^n\right)^2}{\Delta t}+\frac{\partial \rho u_j^m\left(u_i^m\right)^2}{\partial x_j},
\end{aligned} \tag{2.16}$$

which is equivalent to its analytic counterpart Eq. (2.13). This results in an improved stability because the convective term has no effect on $\iiint \rho u_i^2 dV$. This method is also applicable to the scalar conservation.

In the time-staggered scheme used in the present study, a minor modification results in the same conclusion:

$$\begin{aligned}
&2u_i^m\left[\frac{\rho^{n+1}u_i^{n+1}-\rho^n u_i^n}{\Delta t}+\frac{\partial (\rho u_j)^* u_i^m}{\partial x_j}\right]\\
&=\frac{\rho^{n+1}\left(u_i^{n+1}\right)^2-\rho^n\left(u_i^n\right)^2}{\Delta t}+\frac{\partial (\rho u_j)^*\left(u_i^m\right)^2}{\partial x_j},
\end{aligned} \tag{2.17}$$

where

$$u_i^m=\frac{\sqrt{\rho^{n+1}}u_i^{n+1}+\sqrt{\rho^n}u_i^n}{\sqrt{\rho^{n+1}}+\sqrt{\rho^n}},\quad (\rho u_j)^*=\frac{\Delta t_s^+\left(\rho u_j\right)^{n+1}+\Delta t_s^-\left(\rho u_j\right)^n}{2\Delta t},$$

$$\rho^{n+1}=\frac{\rho^{n+\frac{3}{2}}+\rho^{n+\frac{1}{2}}}{2},\quad \rho^n=\frac{\rho^{n+\frac{1}{2}}+\rho^{n-\frac{1}{2}}}{2},$$

$$\frac{\rho^{n+\frac{3}{2}}-\rho^{n+\frac{1}{2}}}{\Delta t_s^+}+\frac{\partial\left(\rho u_j\right)^{n+1}}{\partial x_j}=0, \quad \frac{\rho^{n+\frac{1}{2}}-\rho^{n-\frac{1}{2}}}{\Delta t_s^-}+\frac{\partial\left(\rho u_j\right)^{n}}{\partial x_j}=0.$$

Δt_s is the time step for integrating the scalar (e.g., density and energy) equations. For a conserved scalar f, the modified Crank-Nicolson method becomes

$$\begin{aligned} & 2f^m\left[\frac{\rho^{n+\frac{3}{2}}f^{n+\frac{3}{2}}-\rho^{n+\frac{1}{2}}f^{n+\frac{1}{2}}}{\Delta t_s^+}+\frac{\partial(\rho u_j)^{n+1}f^m}{\partial x_j}\right] \\ & =\frac{\rho^{n+\frac{3}{2}}\left(f^{n+\frac{3}{2}}\right)^2-\rho^{n+\frac{1}{2}}\left(f^{n+\frac{1}{2}}\right)^2}{\Delta t_s^+}+\frac{\partial(\rho u_j)^{n+1}\left(f^m\right)^2}{\partial x_j}, \end{aligned} \tag{2.18}$$

where

$$f^m=\frac{\sqrt{\rho^{n+\frac{3}{2}}}f^{n+\frac{3}{2}}+\sqrt{\rho^{n+\frac{1}{2}}}f^{n+\frac{1}{2}}}{\sqrt{\rho^{n+\frac{3}{2}}}+\sqrt{\rho^{n+\frac{1}{2}}}}.$$

2.5. *Spatial discretization with a conservation property*

Another component for improved stability is a spatial discretization scheme maintaining a feature of the analytic differential operators. This scheme was proposed by Morinishi *et al.* (1998) for incompressible flows and extended to low Mach number flows by Desjardins *et al.* (2008). It is composed of a set of differential and interpolation operators specially designed for conserving the kinetic energy. The key feature of this method is that a skew-symmetric matrix is produced when the convective/advective terms in Eqs. (2.1)−(2.4) are discretized. Using linear algebra, it can be shown that

$$\begin{aligned} \{u\}^T[S]\{u\} &= \left(\{u\}^T[S]\{u\}\right)^T \\ &= \{u\}^T[S]^T\{u\} \\ &= -\{u\}^T[S]\{u\} \\ &= 0, \end{aligned} \tag{2.19}$$

where $[S]$ is a skew-symmetric matrix and $\{u\}$ is a solution vector. In Eqs. (2.1)−(2.4), $\{u\}$ is either the velocity, energy or entropy. Therefore, the discretized form of the integrated squared variable can be written as $\{u\}^T[S]\{u\}$. In effect, Eq. (2.19) is equivalent to the statement that the convective/advective terms do not affect the temporal change of the integrated (summated) squared variables. Thus, this discretization method maintains the feature of the original governing equation.

Honein (2005) suggested the skew-symmetric form of the convective term written as

$$\frac{\partial\rho u_j f}{\partial x_j}=\frac{1}{2}\frac{\partial\rho u_j f}{\partial x_j}+\frac{1}{2}\rho u_j\frac{\partial f}{\partial x_j}+\frac{1}{2}f\frac{\partial\rho u_j}{\partial x_j}. \tag{2.20}$$

Honein argued that the integrated squared variable is not spuriously affected by the nonlinear terms with this form. In the present study, this form is not used because the scheme by Morinishi *et al.* (1998) maintains the discrete equivalence between the divergent and skew-symmetric forms of the convective term. In other words, Eq. (2.20) is discretely satisfied.

2.6. *Removal of a physical stiffness from a large density gradient*

A large gradient of the density is often encountered in compressible simulations, e.g., mixing, combustion, shock, etc. A rapid change of the density in time and space can add significant stiffness to the system of the governing equations. Especially for an implicit scheme, stiffness can slow down the convergence speed or sometimes result in a failure. In the present study, a simple diagonal preconditioner has been derived so that a physical stiffness from a large density gradient is efficiently removed. This results in a more robust and faster convergence of the implicit method, as shown in our numerical test.

The identification of the physical stiffness is motivated by the skew-symmetric form of the convective term Eq. (2.20) and a modified version of the temporal derivative:

$$\frac{\partial \rho f}{\partial t} = \frac{1}{2}\frac{\partial \rho f}{\partial t} + \frac{1}{2}\rho\frac{\partial f}{\partial t} + \frac{1}{2}f\frac{\partial \rho}{\partial t}. \tag{2.21}$$

Combining this with Eq. (2.20) results in

$$\frac{\partial \rho f}{\partial t} + \frac{\partial \rho u_j f}{\partial x_j} = \frac{1}{2}\left[\frac{\partial \rho f}{\partial t} + \rho\frac{\partial f}{\partial t} + \frac{\partial \rho u_j f}{\partial x_j} + \rho u_j\frac{\partial f}{\partial x_j} + f\left(\frac{\partial \rho}{\partial t} + \frac{\partial \rho u_j}{\partial x_j}\right)\right],$$

where the last term in the RHS is zero. However, the last term is non-zero during converging iterations and can be very large in specific problems. For example, under the presence of a sharp change of the density (e.g., a flow with shocks and mixing of fluids with a large density difference), the last term can have the size of $\mathcal{O}(f/\Delta x)$. Because this term eventually becomes zero, its effect during convergence is redundant and may only slow down the convergence. Thus, this term is removed here from the transport equation:

$$\frac{\partial \rho f}{\partial t} + \frac{\partial \rho u_j f}{\partial x_j} = \frac{1}{2}\frac{\partial \rho f}{\partial t} + \frac{\rho}{2}\frac{\partial f}{\partial t} + \frac{1}{2}\frac{\partial \rho u_j f}{\partial x_j} + \frac{\rho u_j}{2}\frac{\partial f}{\partial x_j} = 0. \tag{2.22}$$

An interesting feature of this equation is that the last two terms result in a conservative term ($\partial \rho u_j f^2/\partial x_j$) when multiplied by $2f$, which implies that these terms do not spuriously affect the integrated squared variable $\iiint \rho f^2 dV$. When discretized with the scheme by Morinishi *et al.* (1998), these terms become $[S]\{f\}$ where $[S]$ is a skew-symmetric matrix. A weakness of Eq. (2.22) is that f is no longer discretely conserved.

For the temporal conservation of the integrated squared variable, Eq. (2.22) can be combined with the method of Subbareddy & Candler (2009). For the velocity, it becomes

$$\begin{aligned}
&\frac{1}{2}\frac{\partial \rho u_i}{\partial t} + \frac{\rho}{2}\frac{\partial u_i}{\partial t} + \frac{1}{2}\frac{\partial \rho u_j u_i}{\partial x_j} + \frac{\rho u_j}{2}\frac{\partial u_i}{\partial x_j} \\
&\cong \frac{\rho^{n+1}u_i^{n+1} - \rho^n u_i^n}{2\Delta t} + \frac{\rho^{n+1}+\rho^n}{2}\frac{u_i^{n+1}-u_i^n}{2\Delta t} + \left(\frac{u_i^{n+1}+u_i^n}{2} - u_i^m\right)\frac{\rho^{n+1}-\rho^n}{2\Delta t} \\
&\quad + \frac{1}{2}\frac{\partial (\rho u_j)^* u_i^m}{\partial x_j} + \frac{(\rho u_j)^*}{2}\frac{\partial u_i^m}{\partial x_j} \\
&= \frac{\rho^{n+1} + \sqrt{\rho^{n+1}\rho^n}}{2\Delta t}u_i^{n+1} - \frac{\rho^n + \sqrt{\rho^{n+1}\rho^n}}{2\Delta t}u_i^n + \frac{1}{2}\frac{\partial (\rho u_j)^* u_i^m}{\partial x_j} + \frac{(\rho u_j)^*}{2}\frac{\partial u_i^m}{\partial x_j}.
\end{aligned} \tag{2.23}$$

The third term in the second line of Eq. (2.23) is the additional term for the temporal conservation. The definition of u_i^m and $(\rho u_j)^*$ is the same one as in Eq. (2.17). After this study, we found that the last line of Eq. (2.23) is the same as the discrete skew-symmetric form recently proposed by Morinishi (2010). When multiplied by $2u_i^m$, Eq.

(2.23) becomes

$$\frac{\rho^{n+1}\left(u_i^{n+1}\right)^2 - \rho^n\left(u_i^n\right)^2}{\Delta t} + \frac{\partial(\rho u_j)^*\left(u_i^m\right)^2}{\partial x_j}.$$

Thus, the non-linear term does not spuriously affect $\sum \rho u_i^2$.

3. Numerical tests

The stability of the proposed scheme was tested in two canonical problems and compared with existing schemes. In the present study, both the explicit Runge-Kutta (RK) schemes and the implicit Crank-Nicolson (CN) method are considered as the temporal discretization. For the RK methods, a five-stage method by Stanescu & Habashi (1998) and seven-stage method by Allampalli *et al.* (2009) were employed. In all cases, the second-order central difference is used. As the energy variables, the total energy, internal energy and entropy are considered and compared with each other.

3.1. *A translating inviscid vortex*

The first test problem is the inviscid vortex translating in the streamwise direction. This problem has an analytic solution that is valid with zero viscosity and diffusivity. This problem is popular in testing stability of a numerical scheme in a long time period. In the present study, a vortex is located at the center of a periodic box of 16 by 16 in size and translates for 10 pass-through times. The CFL (convective+acoustic) is maintained at $CFL = 2$, which is smaller than 60% of the stability limit of every temporal scheme.

Figure 1 shows time-history of the kinetic energy with different schemes. The kinetic energy remains constant in time in case of the analytic solution. Every simulation stops when it reaches 10 pass-through times or an error occurs (e.g., floating point exception, negative density/pressure, etc.). It is obvious that the cases with the entropy equation Eq. (2.4) are more stable than the other forms of the energy equation. This confirms the conclusion by Honein (2005). The internal energy shows better stability than the total energy. One reason for this is that the analytic velocity of the inviscid vortex problem is divergence-free, which makes the non-conservative term in Eq. (2.3) zero. In the same form of the energy equation, the CN scheme shows better stability than the RK schemes. This implies that the CN scheme produces a smaller dispersive error than the RK schemes aside from the accuracy. For the relationship between the total and internal energies, different interpolation methods for the kinetic energy Eqs. (2.10)−(2.12) are compared in Figure 1 (d). Eq. (2.10) shows the most stable results among them in both implicit and explicit methods, but the difference is not significant except for Eq. (2.12) with the CN method.

Figures 2 and 3 show the contours of the density approximately after 3 and 10 pass-through times. The entropy and internal energy equation results in a much cleaner density field than the total energy equation. Again, the CN scheme produced a smaller dispersive error than the RK schemes.

3.2. *An unsteady viscous shock problem*

In this section, an unsteady viscous shock problem is considered. This problem is difficult in spite of its one-dimensionality, because every flow variable shows a jump across the shock. In the domain of $-8 < x < 8$ in the streamwise direction, the shock front initially located at $x = -4$ moves to the right with unit speed. The upstream/downstream density ratio is 2.667. The Reynolds number (Re) is 200−500 in the present study. The CFL

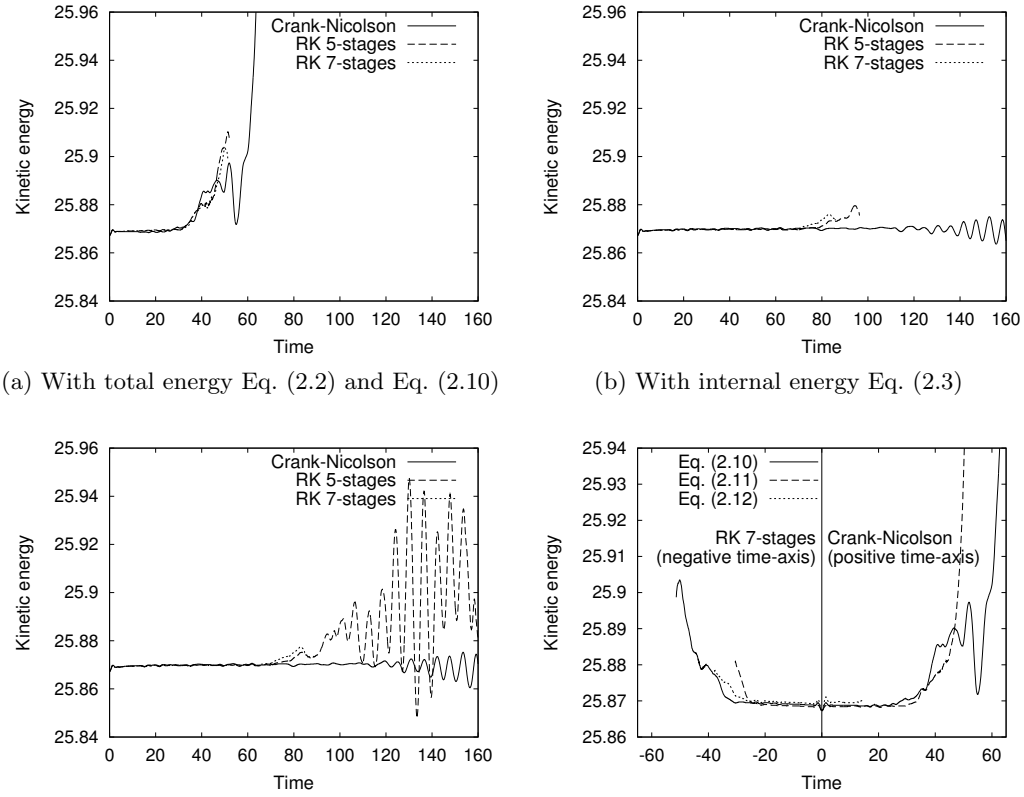

(a) With total energy Eq. (2.2) and Eq. (2.10)

(b) With internal energy Eq. (2.3)

(c) With entropy Eq. (2.4)

(d) With total energy and different interpolations of the kinetic energy

FIGURE 1. Time history of the kinetic energy in the inviscid vortex problem.

number is 1 for Re=200 and 0.5 for Re=500. The number of grid points in the streamwise direction is 96. Because this problem involves a sharp gradient of the density, the modified CN method with the temporal conservation (Subbareddy & Candler 2009) may be useful. In this section, the method proposed in section 2.6 (the temporal conservation + removal of the physical stiffness) is used and compared with the other methods.

Because it is a viscous problem, the governing equations should be in their original forms: i.e.,

$$\frac{\partial \rho u_i}{\partial t} + \frac{\partial \rho u_j u_i}{\partial x_j} = -\frac{\partial p}{\partial x_i} + \frac{\partial \tau_{ij}}{\partial x_j}, \tag{3.1}$$

$$\frac{\partial \rho E}{\partial t} + \frac{\partial u_j \left(\rho E + p\right)}{\partial x_j} = \frac{\partial \tau_{ij} u_i}{\partial x_j} - \frac{\partial q_j}{\partial x_j}, \tag{3.2}$$

$$\frac{\partial \rho e}{\partial t} + \frac{\partial \rho u_j e}{\partial x_j} + p\frac{\partial u_j}{\partial x_j} = \tau_{ij}\frac{\partial u_i}{\partial x_j} - \frac{\partial q_j}{\partial x_j}, \tag{3.3}$$

$$\frac{\partial \rho s}{\partial t} + \frac{\partial \rho u_j s}{\partial x_j} = \frac{1}{T}\left(\tau_{ij}\frac{\partial u_i}{\partial x_j} - \frac{\partial q_j}{\partial x_j}\right), \tag{3.4}$$

where τ_{ij} is the viscous stress tensor and q_i is the thermal heat flux.

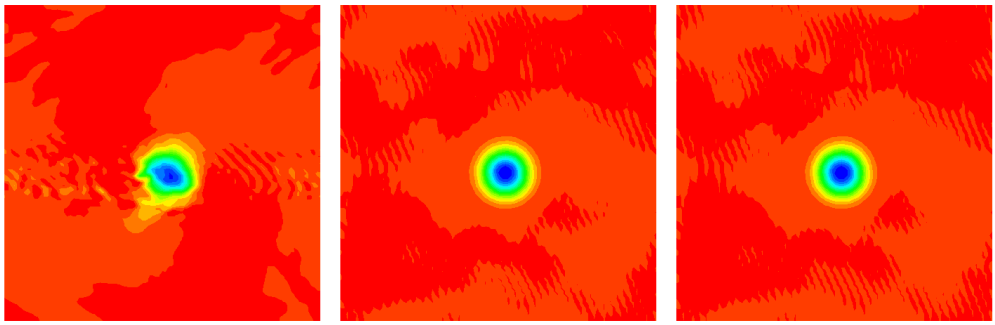

(a) CN with total energy (b) CN with internal energy (c) CN with entropy

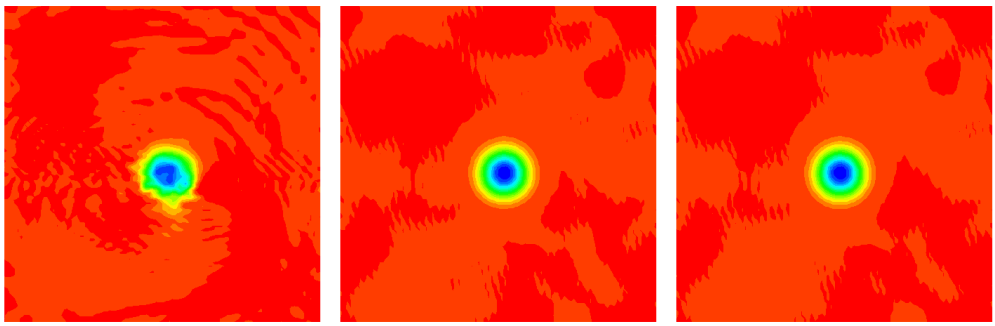

(d) RK7 with total energy (e) RK7 with internal energy (f) RK7 with entropy

FIGURE 2. Contours of the density approximately after 3 pass-through times.

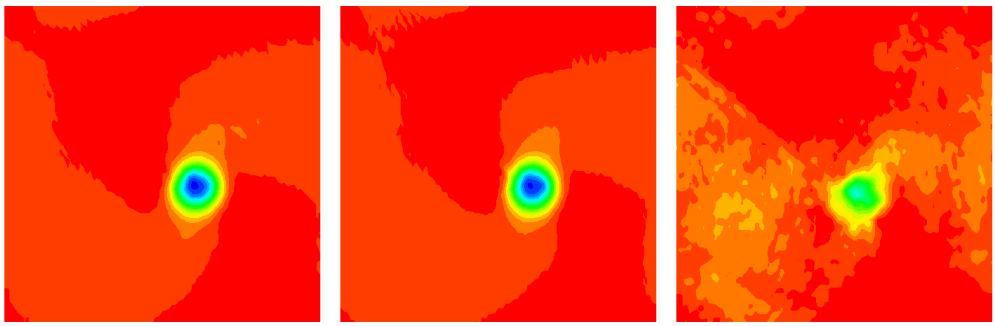

(a) CN with internal energy (b) CN with entropy (c) RK5 with entropy

FIGURE 3. Contours of the density approximately after 10 pass-through times.

First, three interpolation schemes for the kinetic energy Eqs. (2.10)−(2.12) with the total energy Eq. (3.2) are compared with each other. Figure 4 shows the time-history of the minimum and maximum values of the pressure in the entire flow field with the 7-stage RK method at $Re = 200$. It has been observed that the reason for almost all unstable cases in this section is appearance of a negative pressure value from amplification of dispersive errors near the shock. Eq. (2.11) is most stable, which is different from the

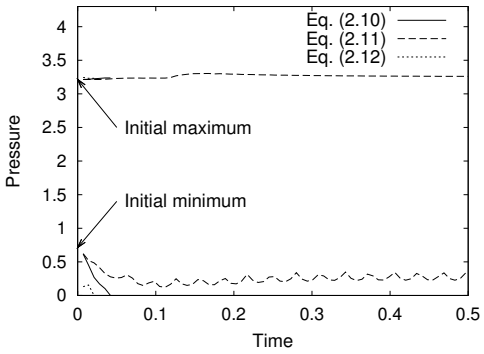

FIGURE 4. Time history of the minimum and maximum pressure with different interpolations for the kinetic energy at $Re = 200$.

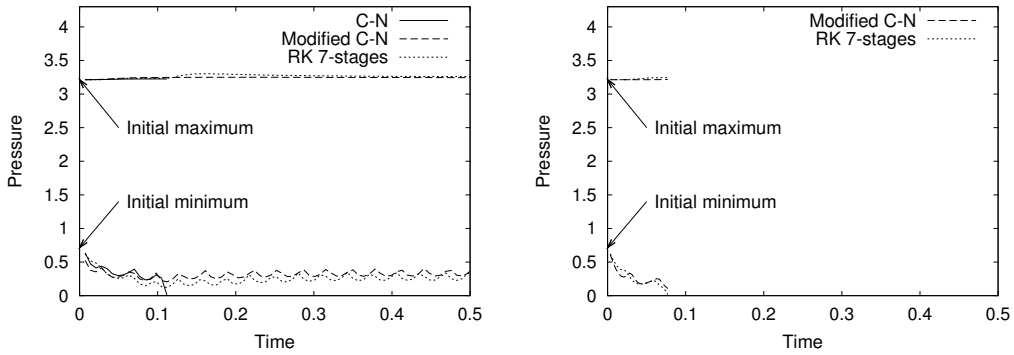

(a) $Re = 200$ (b) $Re = 500$

FIGURE 5. Time history of the minimum and maximum pressure with the total energy Eq. (3.2) and different temporal schemes.

result of the inviscid vortex problem. The optimum method may be problem-dependent and a further study is necessary. The results with the total energy based on Eq. (2.11) are presented below.

Figure 5 shows the results with the total energy Eq. (3.2) and different temporal schemes. For $Re = 200$, only the case with the CN method crashes owing to the negative pressure. This shows that the modified CN method is more robust than the original method. The difference between the minimum pressure and its initial value (shown in the figure) is approximately the maximum size of the dispersive error. The modified CN method produces a smaller dispersive error than the RK method. For $Re = 500$, all methods become unstable as dispersive errors grow.

Figure 6 shows the results with the internal energy Eq. (3.3). A trend very similar to the total energy is observed. In section 2.3, it is argued that, with the spatial discretization of the present study, a sufficient stabilization for only the internal energy equation leads to a stable solution of the momentum equation without additional stabilization. Although this argument is based on the zero-viscosity/diffusivity, its effect is visible by applying the same stabilization to the internal and total energy equations. Figure 7 shows the results with the third-order WENO scheme for only the total and internal energy equations for

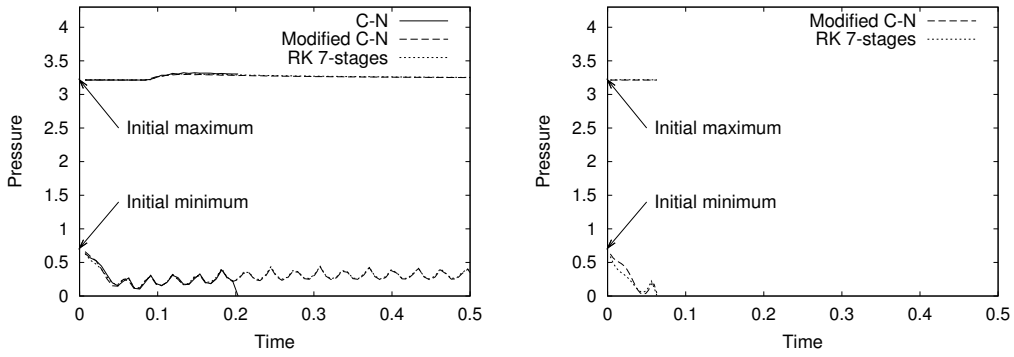

(a) $Re = 200$ (b) $Re = 500$

FIGURE 6. Time history of the minimum and maximum pressure with the internal energy Eq. (3.3) and different temporal schemes.

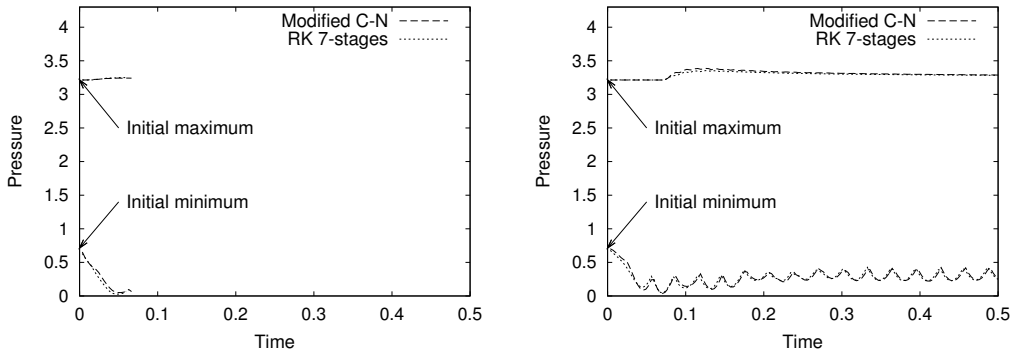

(a) With the total energy (b) With the internal energy

FIGURE 7. Time history of the minimum and maximum pressure with the third-order WENO for the energy equation at $Re = 500$.

the $Re = 500$ cases. The cases with the internal energy become stable, but the cases with the total energy remain unstable. These results suggest that the argument in section 2.3 is valid to some extent in the viscous regime.

Figure 8 shows the results with the entropy Eq. (3.4). With the entropy as the energy variable, all cases with both Reynolds number are shown to be stable. Although it is a viscous problem, this result shows that an improved stability is achieved without artificial stabilization by removing the negative effect of the non-linear terms in the governing equation.

Compared with the original CN method, an advantage of the modified CN method is a faster convergence without a physical stiffness from the continuity equation. For all cases with the modified CN method in this section (not shown in this study but also for the cases of the inviscid vortex), the modified CN method needs about a 20∼30% fewer number of iterations until convergence than the original method does.

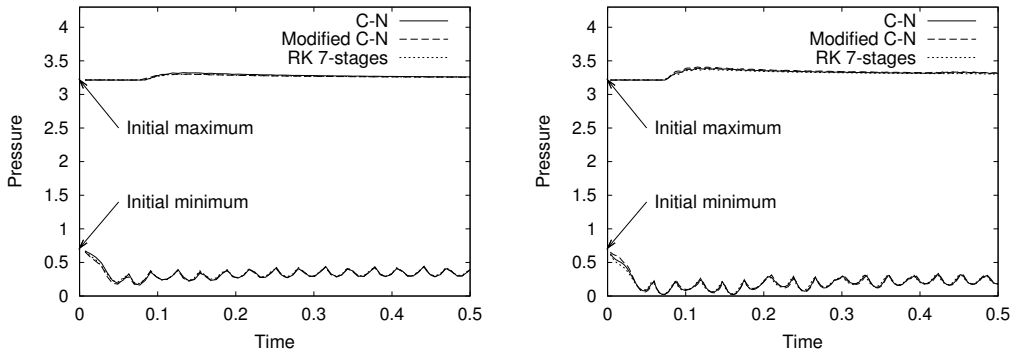

(a) $Re = 200$ (b) $Re = 500$

FIGURE 8. Time history of the minimum and maximum pressure with the entropy Eq. (3.4) and different temporal schemes.

4. Summary

The objective of the present study is to derive a numerical scheme for compressible flows that requires minimum artificial stabilization techniques. First, an analytic relationship between the non-linear terms and the stability is identified. Then, temporal and spatial discretization operators specially designed for a similarity with their analytic counterparts have been combined to obtain discretized governing equations without a spurious effect from the non-linear terms on the integrated squared variables. In order to stabilize convergence of the implicit method for problems with a large density gradient, a simple preconditioning scheme that removes a physical stiffness from the continuity equation was derived. In our numerical tests, the proposed method is shown to be more robust and efficient than the existing methods.

Acknowledgments

Financial support from Center for Turbulence Research (CTR) and NASA is gratefully acknowledged.

REFERENCES

ALLAMPALLI, V., HIXON, R., NALLASAMY, M. & SAWYER, S. D. 2009 High-accuracy large-step explicit Runge-Kutta (HALE-RK) schemes for computational aeroacoustics. *J. Comput. Phys.* **228**, 3837–3850.

DESJARDINS, O., BLANQUART, G., BALARAC, G. & PITSCH, H. 2008 High order conservative finite difference scheme for variable density low mach number turbulent flows. *J. Comput. Phys.* **227**, 7125–7159.

HONEIN, A. 2005 Numerical aspects of compressible turbulence simulations. PhD thesis, Stanford University.

MORINISHI, Y. 2010 Skew-symmetric form of convective terms and fully conservative finite difference schemes for variable density low-Mach number flows. *J. Comput. Phys.* **229**, 276–300.

MORINISHI, Y., LUND, T. S. & OGI, T. 2004 Fully conservative finite difference scheme

in cylindrical coordinates for incompressible flow simulations. *J. Comput. Phys.* **197**, 686–710.

Morinishi, Y., Lund, T. S., Vasilyev, O. V. & Moin, P. 1998 Fully conservative higher order finite difference schemes for incompressible flow. *J. Comput. Phys.* **143**, 90–124.

Pierce, C. D. 2001 Progress-variable approach for large-eddy simulation of turbulent combustion. PhD thesis, Stanford University.

Stanescu, D. & Habashi, W. G. 1998 2N-storage low dissipation and dispersion Runge-Kutta schemes for computational acoustics. *J. Comput. Phys.* **143**, 674–681.

Subbareddy, P. K. & Candler, G. V. 2009 A fully discrete, kinetic energy consistent finite-volume scheme for compressible flows. *J. Comput. Phys.* **228**, 1347–1364.

Wall, C., Pierce, C. D. & Moin, P. 2002 A semi-implicit method for resolution of acoustic waves in low mach number flows. *J. Comput. Phys.* **181**, 545–563.